AEM
Journals.ASM.org

pA506, a Conjugative Plasmid of the Plant Epiphyte *Pseudomonas fluorescens* A506

Virginia O. Stockwell,[a] Edward W. Davis II,[a,b] Alyssa Carey,[a,b] Brenda T. Shaffer,[b] Dmitri V. Mavrodi,[c] Karl A. Hassan,[d] Kevin Hockett,[b]* Linda S. Thomashow,[c,e] Ian T. Paulsen,[d] Joyce E. Loper[a,b]

Department of Botany and Plant Pathology, Oregon State University, Corvallis, Oregon, USA[a]; Agricultural Research Service, U.S. Department of Agriculture, Corvallis, Oregon, USA[b]; Department of Plant Pathology, Washington State University, Pullman, Washington, USA[c]; Department of Chemistry and Biomolecular Sciences, Macquarie University, Sydney, Australia[d]; Agricultural Research Service, U.S. Department of Agriculture, Pullman, Washington, USA[e]

Conjugative plasmids are known to facilitate the acquisition and dispersal of genes contributing to the fitness of *Pseudomonas* spp. Here, we report the characterization of pA506, the 57-kb conjugative plasmid of *Pseudomonas fluorescens* A506, a plant epiphyte used in the United States for the biological control of fire blight disease of pear and apple. Twenty-nine of the 67 open reading frames (ORFs) of pA506 have putative functions in conjugation, including a type IV secretion system related to that of MOB_{P6} family plasmids and a gene cluster for type IV pili. We demonstrate that pA506 is self-transmissible via conjugation between A506 and strains of *Pseudomonas* spp. or the *Enterobacteriaceae*. The origin of vegetative replication (*oriV*) of pA506 is typical of those in pPT23A family plasmids, which are present in many pathovars of *Pseudomonas syringae*, but pA506 lacks *repA*, a defining locus for pPT23A plasmids, and has a novel partitioning region. We selected a plasmid-cured derivative of A506 and compared it to the wild type to identify plasmid-encoded phenotypes. pA506 conferred UV resistance, presumably due to the plasmid-borne *rulAB* genes, but did not influence epiphytic fitness of A506 on pear or apple blossoms in the field. pA506 does not appear to confer resistance to antibiotics or other toxic elements. Based on the conjugative nature of pA506 and the large number of its genes that are shared with plasmids from diverse groups of environmental bacteria, the plasmid is likely to serve as a vehicle for genetic exchange between A506 and its coinhabitants on plant surfaces.

Pseudomonas is a diverse genus of gammaproteobacteria with more than 100 species exhibiting varied lifestyles in a wide range of environments, including soil, water, plant surfaces, and animals. Pseudomonads are well known for their ubiquity in the natural world, their capacity to utilize a striking variety of organic compounds as energy sources, and their resistance to a wide range of medically and agriculturally important antimicrobial compounds. Conjugative plasmids serve important roles in the evolution of these bacteria, facilitating the acquisition and dispersal of genes contributing to their fitness in specific environments. For example, plasmids conferring antibiotic resistance on clinical strains of *Pseudomonas aeruginosa* have been recognized for 4 decades (1) and continue to contribute to the drug tolerance of these bacteria (2). Plasmids are common in strains of the phytopathogenic species *Pseudomonas syringae*, carrying genes for virulence, phytotoxin and phytohormone biosynthesis, UV tolerance, and resistance to copper and antibiotics used in agriculture to control diseases caused by these bacteria (3, 4). Plasmids containing genes for catabolism of pollutants are key to the capacity of certain strains of *Pseudomonas* spp. to function in bioremediation of polluted environments (5). Although plasmids are common in many species of *Pseudomonas* (3, 4), they are far from ubiquitous and appear to be present in only a fraction of strains falling into some taxa, such as the heterogenous *Pseudomonas fluorescens* group. In our recent comparative genomic analysis of 10 strains within this group (6), only one strain, *P. fluorescens* A506, harbored a plasmid.

P. fluorescens strain A506 is a plant epiphyte and a commercial biological control agent (BlightBan A506; NuFarm Americas, Burr Ridge, IL) for management of fire blight, a devastating disease of the Rosaceae caused by *Erwinia amylovora* (7–9). The primary mechanism of disease control ascribed to A506 is competitive exclusion of the pathogen from sites of colonization on the stigmas of flowers (10, 11). In addition to fire blight control, the biocontrol agent also reduces the severity of frost damage caused by ice-nucleation-active bacteria (10). Beyond its commercial applications, A506 has been used as a biosensor of the chemical nature of microbial habitats (12–15) and as a model organism for studies evaluating resource competition (16, 17), survival and growth of bacteria on aerial plant surfaces (8, 9, 18, 19), spatial patterns of bacterial cell aggregates on plants (20, 21), and the viable but nonculturable condition that can occur in bacteria (22, 23).

The goal of this study was to sequence and characterize pA506, the plasmid of strain A506. Here, we provide a comparative analysis of the sequence and describe features of the plasmid, including conjugal transfer; stability; and its role in UV tolerance, twitching motility, and epiphytic fitness of the host bacterium.

MATERIALS AND METHODS

Bacterial strains, plasmids, and general culture conditions. Bacterial strains and plasmids are listed in Table 1. All bacterial strains were stored

Received 29 April 2013 Accepted 21 June 2013
Published ahead of print 28 June 2013
Address correspondence to Joyce E. Loper, Joyce.Loper@ars.usda.gov.
* Present address: Kevin Hockett, The School of Plant Sciences, University of Arizona, Tucson, Arizona, USA.
Supplemental material for this article may be found at http://dx.doi.org/10.1128/AEM.01354-13.

doi:10.1128/AEM.01354-13

TABLE 1 Bacterial strains and plasmids

Strain or plasmid	Relevant traits[a]	Source or reference(s)
Strains		
Pseudomonas spp.		
P. aeruginosa PAO1		75
P. brassicacearum Q8r1-96	Isolated from wheat rhizosphere in Washington, USA; biological control of take-all of wheat; plasmidless	D. Weller (76)
P. chlororaphis O6	Isolated from soil; biological control of multiple biotic and abiotic stresses of plants; plasmidless	A. Anderson (77)
P. fluorescens A506	Isolated from pear phyllosphere in California, USA; registered commercial biological control agent for fire blight; single plasmid, pA506; Rf Sm	10
P. fluorescens A506 pA506::*gfp-km-gm*	Single insertion of *gfp-km-gm* cassette from pTGN in pA506 in PflA506_p0022; GFP^+; Gm Km Rf Sm	This study
P. fluorescens A506-ΔpA506	Plasmidless derivative of A506; Rf Sm	This study
P. fluorescens SS101	Isolated from wheat rhizosphere in The Netherlands; biological control of diseases caused by oomycetes, i.e., *Pythium* and *Phytophthora* species; plasmidless	J. Raaijmakers (78)
Enterobacteriaceae		
Escherichia coli K-12	ATCC 15153, Sm	American Type Culture Collection
E. coli S-17 (λ*pir*)	*pro thi hsdR3M*, RP4-2-Tc:Mu-Km:Tn*7* λ*pir*; Sm	26
Pantoea vagans C9-1	Isolated from apple phyllosphere in Michigan USA; registered biological control agent for fire blight; three large plasmids (pPag1, pPag2, pPag3)	79, 80
Plasmids		
pCR2.1-TOPO	pCR2.1-TOPO cloning vector; Km	Invitrogen
pTGN	pBSL202 with mini-Tn*5* *gfp-km-gm*; transposon including a promoterless *gfp*-Km and constitutively expressed Gm	26
pA506::*gfp-km-gm*	Single insertion of *gfp-km-gm* cassette of pTGN in PflA506_p0022	This study

[a] Gm, Km, Rf, and Sm, resistance to gentamicin, kanamycin, rifampin, and streptomycin, respectively.

at −80°C in nutrient broth with 15% glycerol. Pseudomonads were cultured routinely on LB (24) or King's medium B (KB) (25) at 27°C, and *Escherichia coli* and *Pantoea vagans* were cultured on LB at 37°C, unless specified otherwise. Cycloheximide, kanamycin, rifampin, and streptomycin (Sigma Chemical Co., St. Louis, MO) were each used at 50 μg/ml, unless specified otherwise, and gentamicin was used at 40 μg/ml.

Plasmid mutagenesis and eviction. A derivative of pA506 having an insertion of the *gfp-km-gm* mini-Tn*5* (i.e., pA506::*gfp-km-gm*) was obtained following transposon mutagenesis of A506. A mini-Tn*5* *gfp-km-gm* cassette on pTGN (26) was introduced into A506 by conjugative transfer. Random insertion mutants were selected on KB amended with rifampin and gentamicin. One mutant that originally exhibited the green fluorescence and gentamicin resistance conferred by *gfp-km-gm* mini-Tn*5* subsequently lost these phenotypes following repeated transfer on KB. DNA was isolated from the original mutant and from derivatives that lost the green fluorescent protein (GFP) fluorescence and antibiotic resistance. This DNA was evaluated by gel electrophoresis, and results showed that pA506 was present in the original mutant but absent from the derivative strains (data not shown). The lack of pA506 in the derivative strains was confirmed by PCR using primers specific to plasmid-borne genes (see Table S1 in the supplemental material), and one of the plasmidless derivative strains (A506-ΔpA506; Table 1) was selected for use in this study. Plasmid DNA from the original GFP-positive, gentamicin-resistant mutant was isolated using a modified alkaline lysis procedure (24), and the location of the *gfp-km-gm* cassette in pA506::*gfp-km-gm* was determined by inverse PCR. Briefly, plasmid DNA was digested with PstI or NcoI, both of which cut within *nptII* of mini-Tn*5* *gfp-km-gm*. The enzymes were inactivated, and the digested DNA was circularized by self-ligation. Ligation products were used as the templates for amplification of DNA flanking the mini-Tn*5* *gfp-km-gm* using outward-facing, transposon-specific primers (see Table S1). The PstI ligation product contained DNA adjacent to *gfp*, and the NcoI ligation product contained DNA adjacent to *gm*. The PCR products were isolated and sequenced, and the sequence was compared to that of pA506. Sequence analysis of the PCR products showed that the *gfp-km-gm* cassette had inserted in the plasmid at locus PflA506_p0022 (A506 pA506::*gfp-km-gm*; Table 1). Cell morphology of 24-h and 48-h LB and KB broth cultures of A506, A506-ΔpA506, and A506 pA506::*gfp-km-gm* was examined with a Leica DM LS2 microscope equipped with a Leica DFC320 digital camera. Digital images were viewed on a computer screen, and cell lengths were measured. At each time point, 60 cells from three replicate cultures of each strain were measured. The experiment was repeated once. Mean cell lengths were calculated, and Fisher's least significant difference ($P = 0.05$) was used for mean separation.

Sequencing pA506. The sequence of pA506 was obtained during a comparative genomics project of several strains of *Pseudomonas* spp. with biological control activity (6). The pseudomonads, including A506, were sequenced using a combination of Sanger sequencing (to 4× coverage of the genome) and 454 pyrosequencing technologies with paired end reads and assembled as described previously (6). Gaps were closed by merging overlapping contigs and resolving repetitive gaps and sequencing of PCR amplicons between the remaining gaps. The sequence of pA506 is available through NCBI (accession CP003042).

Bioinformatic analysis. Identification of putative genes and annotation of the plasmid were performed as previously described (6). A phylogenetic analysis of each gene was performed with a combination of position-specific iterative (PSI) BLAST search and Clustal Omega alignment (27) on the EBI website (https://www.ebi.ac.uk/Tools/msa/clustalo/). Phylogenetic trees were generated with FastTree 2 (28). Genes selected for further analysis were analyzed with a combination of a BLASTP search to identify homologous genes for use in tree construction and the L-INS-I method in MAFFT 7 (29) for alignment. Substitution models were chosen according to BIC in ProtTest 3 (30). Phylogenetic trees were constructed using RAxML 7.4.2 (31) (20-maximum-likelihood [ML] search with rapid hill-climbing and 1,000 rapid bootstraps [setting f a]) and raxmlGUI (32) in some cases. MEGA 5 (33) and TreeGraph 2 (34) were used to visualize alignments and trees.

Plasmids within the MOB_{P6} family (35) were identified by BLASTP

searches with relevant genes from the NCBI database. Specifically, the first 360 amino acids (aa) of the relaxase protein (PflA506_p0066) were used in a BLASTP search with the query "plasmid" as a filter. A drastic drop-off in E value was noted after 4e−43; proteins under this threshold and previously identified members of the MOB_{P5} and MOB_{P7} groups were used in construction of the relaxase tree. For analysis of *oriV*, *oriT*, and *par* regions, the plasmid was visualized using UGENE and searched for repeats, inverted repeats, and DnaA boxes (36). *oriT* and *oriV* alignments were performed with MUSCLE (37) and examined with Jalview 2 (38).

Determining the origin of replication. Sequence analysis indicated that the origin of replication of pA506 may comprise a region near PflA506_p0001. Segments of a 2,218-nucleotide (nt) region (nt 56556 to nt 1797) spanning the predicted origin region of pA506 were amplified using primer sets in Table S1 in the supplemental material. The amplicons ranged from 440 to 2,003 nt, and each was cloned into pCR2.1-TOPO according to the manufacturer's guidelines (Invitrogen, Grand Island, NY). The inserts in pCR2.1-TOPO (Table 1) were confirmed by sequencing by the CGRB Core lab of Oregon State University.

The pCR2.1-TOPO constructs and the pCR2.1-TOPO vector alone were introduced into A506-ΔpA506 by electroporation. Electrocompetent cells of A506-ΔpA506 were prepared from 24-h cultures on fresh, solidified LB medium. Cells were washed three times with ice-cold 10% glycerol and kept on ice until electroporation. Forty nanograms of each plasmid was combined with electrocompetent cells in a 0.2-cm cuvette with a Bio-Rad Gene Pulser Xcell at 2,500 V, 25 μF, and 200 Ω (Bio-Rad, Hercules, CA). Cells were immediately suspended in LB broth, incubated for 2 h at 27°C with gentle shaking, and then spread on solidified LB amended with kanamycin. The maintenance of pCR2.1-TOPO constructs in A506-ΔpA506 was evaluated by culturing transformants in LB broth at 27°C over 100 generations and then spreading the cultures on solidified LB and LB amended with kanamycin. The presence of the pCR2.1-TOPO construct in five kanamycin-resistant colonies was confirmed with the PCR using primers targeted to the cloned region of the putative origin of replication of pA506.

Conjugal transfer of pA506 to pseudomonads and enteric bacteria. A506 (pA506::*gfp-km-gm*) was used as a donor to track conjugal transfer of pA506. Bacteria were grown with agitation in KB broth; gentamicin was added to cultures of the donor strain. Cells in late log phase (18 to 24 h) were harvested by gentle centrifugation and washed with KB broth. Donor and recipient strains were mixed and placed on a sterile 0.45-μm filter disc (Millipore Corporation, Bedford, MA) on a mating medium that contained (for 1 liter): 1.5 g K_2HPO_4, 5 g yeast extract, 10 g peptone, 5 g glucose, 2.5 g NaCl, and 15 g agar (39). After incubation at 20°C for 24 h, cells were washed from filters and cell suspensions were spread on a selective medium. For experiments evaluating pA506::*gfp-km-gm* transfer to *Pseudomonas* spp., transconjugants were selected on 925 minimal medium (40) containing 0.1% (wt/vol) sodium benzoate as the sole carbon source and gentamicin. Recipient strains *P. fluorescens* SS101, *Pseudomonas brassicacearum* Q8r1-96, and *Pseudomonas chlororaphis* O6 can utilize sodium benzoate as a sole carbon source, whereas A506 cannot (6). For experiments evaluating pA506::*gfp-km-gm* transfer to *E. coli* or *P. vagans*, transconjugants were selected on KB amended with gentamicin incubated at 41°C (*E. coli* K-12) or 37°C (*P. vagans* C9-1), as the donor strain A506 does grow at these high temperatures. The conjugal transfer experiments were repeated four times.

Putative transconjugants were examined for GFP fluorescence with a hand-held UV lamp and tested with PCR primers designed to amplify a unique region of the chromosome of A506 (see Table S1 in the supplemental material). A modified alkaline lysis method was used to isolate plasmid DNA from putative transconjugants (24). The isolated plasmids were digested with BamHI, and fragments were examined with agarose gel electrophoresis.

Twitching motility assay. A506, A506-ΔpA506, and *P. aeruginosa* PAO1 were tested for twitching motility at 27°C (41). Cells of strains were stab inoculated with a sterile toothpick onto solidified KB with 1% agar. Colony diameter was measured periodically, up to 48 h. Motility experiments were conducted four times.

Tolerance to UV irradiation. The method of Whistler et al. (42) was used to evaluate tolerance of strains to UVC irradiation. A506, A506-ΔpA506, *P. fluorescens* SS101, *P. brassicacearum* Q8r1-96, and *P. chlororaphis* O6 were cultured in LB broth to early stationary phase, and dilutions were spread on solidified KB. Plates were immediately placed in a laminar flow hood (SterilGard III; The Baker Company, Sanford, ME) with a germicidal lamp and exposed for 0 to 100 s to UVC irradiation (λ = 254 nm) at a level of 2 J/m^2 per s. After exposure, plates were incubated in darkness, to minimize photoreactivation, and after 3 days, colonies were counted. UVC tolerance experiments were repeated four times.

Epiphytic fitness of A506 and A506-ΔpA506 on flowers. Epiphytic fitness of strains A506 and A506-ΔpA506 was estimated on flowers of pear (*Pyrus communis* L. 'Bartlett') and apple (*Malus x domestica* Borkh., 'Gala' and 'Red Delicious') in experimental orchards at the Oregon State University Botany and Plant Pathology Field Laboratory near Corvallis, OR. Weather data for field trials are summarized in Table S2 in the supplemental material. An aqueous suspension of each strain (1×10^8 CFU/ml) was sprayed at near-full bloom on blossom clusters on marked branches of four replicate trees arranged in a randomized complete block design. Within blocks, treated trees were separated by at least two nontreated trees. At each sampling date, culturable bacterial populations were estimated from 10 individual flowers harvested from each replicate tree using previously described methods (43). Flowers were washed with phosphate buffer, and washes and dilutions were spread on *Pseudomonas* agar F (Difco Laboratories, Detroit, MI) amended with cycloheximide and rifampin. Colonies were enumerated after 3 days. On the final sample date of each experiment, eight randomly selected colonies of A506 were tested for pA506 with a PCR assay. Mean population size of bacterial strains and standard error were calculated by averaging the logarithm (base 10) of population values. The detection limit was 1×10^2 CFU/flower.

Nucleotide sequence accession number. The sequence of pA506 is available through NCBI (accession no. CP003042).

RESULTS AND DISCUSSION

General overview of plasmid pA506. pA506 is a 56,977-bp circular plasmid with 67 predicted coding sequences (CDSs) having putative functions in plasmid replication, maintenance and stability, conjugal transfer, and epiphytic fitness (Fig. 1; see also Table S3 in the supplemental material). The average G+C content (52%) of the plasmid differs from that of the chromosome of *P. fluorescens* A506 (61%) (6), which is not uncommon for extrachromosomal self-replicating elements. The G+C content also varies within the plasmid (Fig. 1), and these local changes in nucleotide composition are likely to correlate with regions of sequence derived from distinct origins.

pA506 shares many genes with members of the well-characterized pPT23A plasmid family, such as pPSR1 from *P. syringae* pv. syringae A2 (44), pMA4326A from *P. syringae* pv. maculicola (4), and the small plasmid from *P. syringae* pv. phaseolicola 1448A (45) (Fig. 1; see also Fig. S1 in the supplemental material). Plasmids in the pPT23A family are self-transmissible and stably maintained in *Pseudomonas* spp. (3, 46), and so it is plausible that such plasmids could be exchanged readily among bacteria coinhabiting aerial plant surfaces, such as A506 and the pathovars of *P. syringae* known to harbor these plasmids. A large fraction of pA506 is similar to regions in pEU30, a plasmid found in some isolates of *E. amylovora* from the western United States (47), and pET49 of *Erwinia tasmaniensis* (48). *E. amylovora* causes fire blight disease of pome fruits, the target disease for biological control by A506, and inhabits floral tissues of pear, the host from which A506 was isolated. *E. tasmaniensis* also exists as an epiphyte on pear and

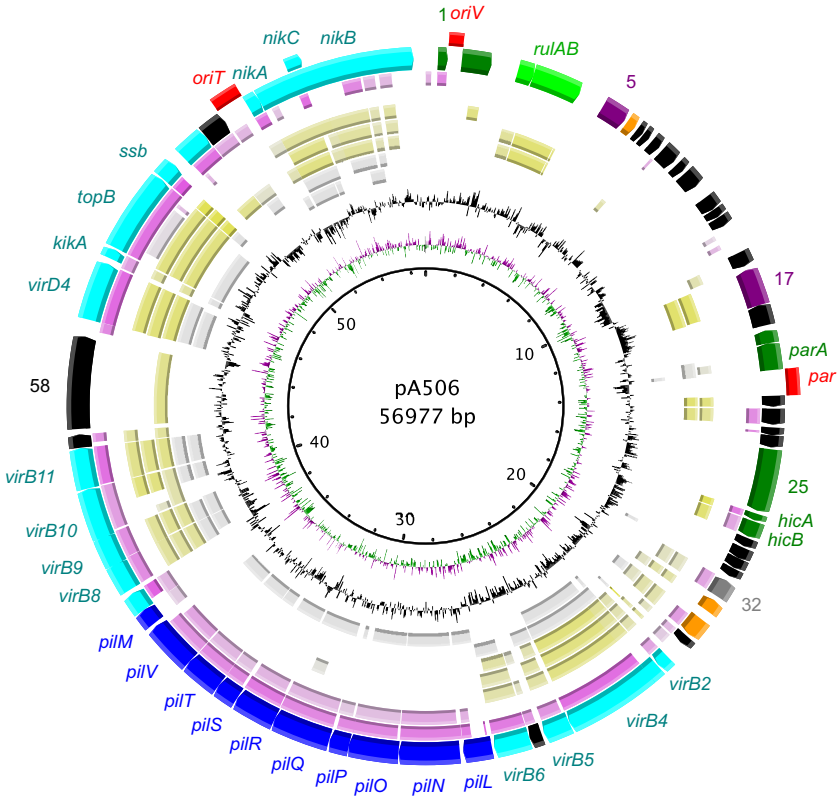

FIG 1 Map of pA506. The outer circle shows predicted coding sequences color coded by putative function: dark green, plasmid replication and stability; green, UV resistance; purple, site-specific recombinases; orange, regulation; black, hypothetical proteins; gray, pyocin immunity protein; blue and turquoise, conjugation. Annotated functions or locus tags (i.e., PflA506_p0001 is shown as 1) are shown outside the circle. Intergenic regions with putative functions as the origin of transfer (*oriT*), origin of vegetative replication (*oriV*), and partitioning centromere (*par*) are shown in red. Circles 2 through 8 depict regions of pA506 that are conserved in seven other plasmids as determined by tBLASTn (cutoff of 1e−5). Second circle (lavender), pMPR124 from *P. fluorescens*; third circle (lavender), PAPI-1 from *P. aeruginosa* PA14; fourth circle (yellow), pMA4326A from *P. syringae* pv. maculicola; fifth circle (yellow), pPSR1 from *P. syringae* pv. syringae; sixth circle (yellow), the small plasmid from *P. syringae* pv. phaseolicola 1448; seventh circle (gray), pEU30 from *E. amylovora*; eighth circle (gray), pET49 from *E. tasmaniensis*. Within each circle, the darkest color indicates nucleotide identity exceeding 40% whereas the lightest color represents identity exceeding 20%. Ninth circle, G+C content. Tenth circle, GC skew. Eleventh circle, coordinates in kilobase pairs. The circular plasmid diagram was generated using BRIG (74).

apple but does not cause fire blight (48). Again, it is plausible that plasmids could be exchanged between these bacteria on plant surfaces. pA506 also shares a large proportion of its gene inventory with certain integrated conjugative elements (ICEs) of *Pseudomonas* spp. (49, 50); although these elements are typically associated with the bacterial chromosome, they are known to be self-transmissible elements that can replicate autonomously (50). Of the plasmid sequences currently available in NCBI, pA506 is most similar to pMP-R124, a 43,794-bp plasmid in a strain of *P. fluorescens* isolated from a cave (accession number NZ_CM001562.1). Despite its similarities to components of each of these plasmids, pA506 has a unique combination of genes and features that distinguishes it from plasmids previously described in the literature. The cargo genes of pA506 include a putative pyocin immunity protein which is unlinked to any pyocin gene and is most similar to pyocin S3 immunity protein from *P. aeruginosa* PA14 (51). This immunity protein could protect A506 from pyocins produced by other bacteria in the environment. A large percentage (39%) of the predicted coding sequences on pA506 encode proteins of unknown function, many with little or no sequence identity to other proteins currently included in the NCBI database. Ten of these are flanked by integrases typically associated with phage integration but are otherwise distinct from any characterized phage genes described in the literature to date.

Plasmid replication and partitioning. A bioinformatic analysis of pA506 revealed a 191-nt sequence similar to the origin of vegetative replication (*oriV*) of pPSR1 and many other plasmids in the pPT23A family (44) (Fig. 2; see also Fig. S2 in the supplemental material). Plasmid *oriV* sequences typically include binding sites for the host chromosomal replication initiation protein DnaA, and the 191-nt sequence includes a putative DnaA box, which differs by 1 nucleotide from the consensus DnaA binding site (52). The predicted secondary structure of the 191-nt sequence contains a hairpin loop that is also present in the *oriV* of pPSR1 (44) and characteristic of *oriV* sequences of many plasmids. Despite these similarities, pA506 lacks *repA*, which is adjacent to *oriV* in all known plasmids in the pPT23A family (46) and has been shown to be required for replication of pPSR1 (44). Adjacent to *oriV*, however, is a gene (PflA506_p0001) that is 58% identical at the amino acid level to *repB*, which is required for replication of pRA2 in *Pseudomonas alcaligenes* (53). pA506 lacks other genes required for replication that are adjacent to *repB* in pRA2 and does not have a region similar to the described *oriV* of pRA2, suggesting that mechanisms of replication are not conserved between the two

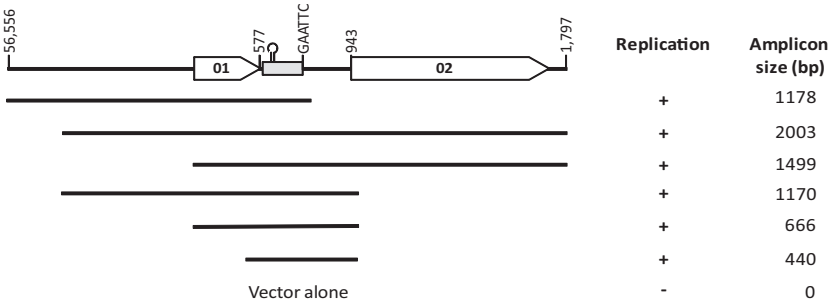

FIG 2 Identification of *oriV* of pA506. A map of the region of pA506 extending from coordinate 56556 to 1797 is shown, with coding sequences for PflA506_p0001 (01) and PflA506_p0002 (02) depicted as arrows and intergenic regions depicted as a black line. A 190-bp region conserved with pPSR1 is shown as a gray box, and a sequence that could form a stem-and-loop structure is also shown. Black lines below the map show the sequences that were cloned in pCR2.1-TOPO. The ability of the clones to replicate in A506Δ-pA506 and the sizes of the cloned sequences are shown. The recircularized pCR2.1-TOPO vector did not replicate in A506Δ-pA506.

plasmids. Homologs of PflA506_p0001 are present in a number of plasmids in the *Enterobacteriaceae* and in pPT14-32 from *P. syringae* (see Fig. S3), but are not present in pPT23A family plasmids that have been characterized to date. To determine if the putative *oriV* and PflA506_p0001 were required and sufficient for pA506 replication, we amplified and cloned DNA fragments from the region into the pCR2.1-TOPO plasmid, which did not replicate in A506-ΔpA506. The recombinant plasmids were introduced into A506-ΔpA506 through transformation (Fig. 2). A 440-nt fragment encompassing the intergenic region between PflA506_p0001 and PflA506_p0002 was sufficient for replication of the recombinant plasmid in A506-ΔpA506. Furthermore, the recombinant plasmid containing the 440-nt insert was maintained by A506-ΔpA506 following growth without antibiotic selection for at least 100 generations (data not shown), indicating that the plasmid was stably maintained in this bacterium. The stable maintenance of the plasmid suggests that the *oriV*s of pA506 and pCR2.1-TOPO are compatible and that the combined replicons may constitute a framework for construction of shuttle vectors useful in the pseudomonads and *Enterobacteriaceae*. The 440-nt fragment did not contain PflA506_p0001 or any other predicted CDSs, which suggests that the replicative machinery in the host bacterium was sufficient for plasmid replication. Although plasmid replication commonly requires plasmid-encoded replicases (44), this is not always the case. For example, the replicative enzyme RepA is not required for replication of the plasmid pRK2 in *Pseudomonas* spp. but is required for pRK2 replication in *E. coli* (52). pA506 also replicates in the enterobacterial species *E. coli* (data not shown) and *P. vagans* (Fig. 3), and we cannot exclude the possibility that genes or sequences outside the 440-nt region required for replication in A506-ΔpA506 are needed for replication in those bacteria. For example, the 628-nt intergenic region between *nikB* and PflA506_p0001 (Fig. 1) has some characteristics of a plasmid replication origin, including A+T-rich repeats that typically serve as binding sites for host replication initiation factors, two 8- and 9-bp inverted repeats, and 16 putative DnaA boxes, which differ by 2 nucleotides from the consensus sequence (data not shown). It is possible that this intergenic region or other components of pA506 are involved in replication of the plasmid in some bacterial hosts.

Large plasmids (exceeding 30 kb in size), such as pA506, are typically maintained at low copy number in the bacterial cell (54). Such low-copy-number plasmids depend on partitioning systems to ensure their stable inheritance by daughter bacterial cells. The partitioning loci (*par*) typically consist of three elements: (a) a centromere-like site containing a series of small nucleotide repeats; (b) a centromere-binding factor, which forms a nucleoprotein complex with the centromere; and (c) an ATPase or GTPase that interacts with the centromere-binding factor to assemble a structure that ensures the distribution of the plasmids between dividing bacterial cells (55, 56). Typically, genes encoding the two protein components are clustered with the centromere-like site on a plasmid. Plasmid centromeres and centromere-binding factors are quite diverse, but genes encoding the ATPase/GTPase component fall into distinct groups. Most plasmid partitioning systems use ATPases in the ParA family (55, 56), and a member of this protein family, PflA506_p0020, is present in pA506. PflA506_p0020 is adjacent to an intergenic region having sets of repeated sequences separated by spacer sequences, which is characteristic of the centromere-like element of partitioning systems (55, 56). Within the intergenic region between PflA506_p0020 and PflA506_p0021 are 24 repeats with a GAATTC consensus sequence distributed over 313 nt (Fig. 4). The repeats are organized into four sets of three to nine repeats, each separated by 4- to 7-nt spacers having low (38%) G+C content. Each of the four sets is separated by 18-nt spacers. Although the number and specific

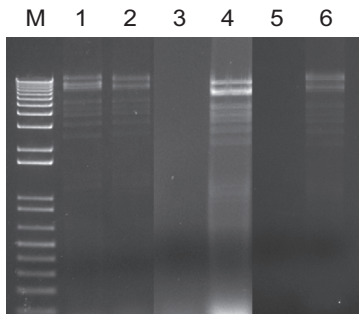

FIG 3 Evidence for conjugative transfer of pA506 from A506 to *Pseudomonas fluorescens* SS101 and *Pantoea vagans* C9-1 and maintenance of pA506 in those bacterial hosts. BamHI digest of plasmids isolated from wild-type strains and recipients with pA506::*gfp-km-gm*. Lanes: M, 1-kb plus marker; 1, pA506; 2, pA506::*gfp-km-gm*; 3, *P. fluorescens* SS101; 4, *P. fluorescens* SS101 pA506::*gfp-km-gm*; 5, *P. vagans* C9-1; 6, *P. vagans* C9-1 pA506::*gfp-km-gm*. *P. fluorescens* SS101 does not have a plasmid. *P. vagans* C9-1 has 3 megaplasmids that were not isolated with the alkaline lysis method.

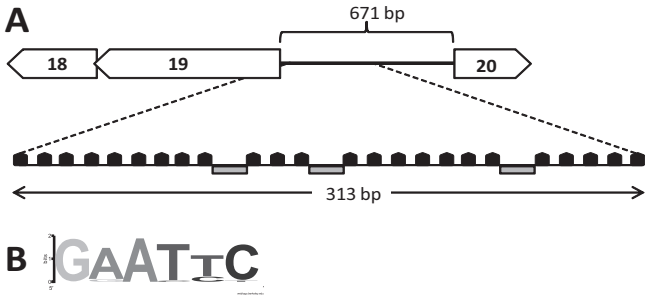

FIG 4 The putative partitioning region of pA506. (A) A map of the region of pA506 extending from coordinates 12602 to 14265 is shown, with coding sequences depicted as open arrows and the intergenic regions depicted as a black line. The enlargement shows 313 bp of the intergenic region between PflA506_p0020 and PflA506_p0021. Each pentagon represents one of the repeated six-nucleotide sequences (GAATTC) present in the region, which are separated by 4- to 7-bp spacer sequences with low G+C content. Three longer 18-bp spacer sequences with low G+C content (35 to 39%) are depicted with shaded boxes. (B) The sequence motif logo was generated from the conserved six-nucleotide repeat regions depicted as pentagons in panel A (http://weblogo.berkeley.edu/).

sequences of repeats in the putative *par* region of pA506 differ from those in known *par* regions, the centromere-like elements of plasmid partitioning systems are known to be diverse in sequence, with the common feature being the presence of many short nucleotide repeats that are key to the formation of secondary structures necessary for proper partitioning of the plasmid (55, 56). In pA506, there are 15 GAATTC repeats outside the intergenic *par* region, with one bordering the putative *oriV* (Fig. 2) and the other 14 in an apparently random distribution throughout the plasmid. The role, if any, of these dispersed repeats is unknown. The third element of the plasmid partitioning system of pA506 may be encoded by PflA506_p0019, although the sequence of this gene exhibits little similarity to characterized centromere-binding factors. In the large plasmid of *P. syringae* pv. phaseolicola 1448A, homologs of PflA506_p0020 and PflA506_p0019 are adjacent to one another and to a putative centromere-like region, having 16 direct repeats with a GAWWTC consensus sequence and 5- to 6-nt low-G+C (32%) spacers (45). Homologs are also present in pPT14-32 of *P. syringae* and other plasmids from *P. syringae* and several species of alphaproteobacteria (see Fig. S4 in the supplemental material). Nevertheless, the putative *par* loci of pA506 are distinct from the plasmid partitioning systems that have been characterized to date.

Plasmid stability is commonly promoted by postsegregation killing systems called toxin-antitoxin systems, which are composed of a stable toxin and an unstable antitoxin. pA506 contains putative genes for a toxin-antitoxin system in the HicAB family, which is widely distributed in bacteria and archaea (57). In *E. coli*, *hicA* encodes an inhibitor of translation and *hicB* encodes a protein that neutralizes HicA (58). The *hicAB* loci of pA506 are most closely related to those in plasmid pMA4326A of *P. syringae* pv. maculicola but are also related to those in the chromosomes of *Pseudomonas* spp. (see Fig. S5 in the supplemental material).

As defined above, the putative partitioning region of pA506 extends from PflA506_p0019 to PflA506_p0027 (*hicB*) and includes four CDSs annotated as hypothetical proteins. Two of these (PflA506_p0021 and PflA506_p0022) are also present in several of the pPT23A family plasmids, including pPSR1 and pPMA4326A (Fig. 1). PflA506_p0022 was disrupted by insertion of mini-Tn*5-gfp-km-gm* following random transposon mutagenesis, and we observed that the resulting plasmid (pA506::*gfp-km-gm*) was not stably maintained by A506. After serial passage in KB for 100 generations without selection, pA506 was retained by >95% of the cells, but only 0.01 to 0.0001% of cells of A506 pA506::*gfp-km-gm* were resistant to kanamycin (data not shown). The kanamycin-resistant cells had retained the marked plasmid; they were GFP^+ and resistant to gentamicin, and the *oriV* of pA506 was detected with PCR (data not shown). Cells of A506 pA506::*gfp-km-gm* had an altered morphology compared to those of A506 and A506-ΔpA506 (see Fig. S6 in the supplemental material). The mean cell lengths of A506 and A506-ΔpA506 were not significantly different from one another ($P = 0.05$) in LB or KB broth culture at 24 or 48 h. In contrast, cells of A506 pA506::*gfp-km-gm* exhibited filamentous growth and, on average, were 4.1 times (24 h) and 4.6 times (48 h) longer ($P < 0.0001$) than those of A506 and A506-ΔpA506 in either medium. Changed cell morphology due to mutagenesis of *par* has been observed with other bacteria. For example, disruption of chromosomal *parA* or *parB* in *P. aeruginosa* resulted in filamentous cell morphology (59). It is possible that the transposon insertion into PflA506_p0022 had a polar effect on the downstream gene, PflA506_p0023. These data suggest that one or both of these genes, which are not closely related to any genes of known function, are involved in plasmid stability or segregation and that their disruption can alter cell morphology.

Conjugal transfer genes of pA506. Plasmid conjugation is typically mediated through a type IV secretion system composed of a channel spanning the bacterial membrane and a pilus that contacts the recipient cell (60). The conjugal transfer region of pA506, which extends from PflA506_p0036 to PflA506_p0067, has nearly all components of this type IV secretion system as well as a set of *pil* genes for type IV pilus biogenesis. PflA506_p0066 encodes a putative relaxase, the enzyme that catalyzes the initial cleavage of DNA at the *nic* site within the origin of transfer (*oriT*) region of the plasmid to produce the single-stranded DNA that is transferred to the recipient cell. Due to their key role in plasmid mobility, relaxases have been used as a phylogenetic tool for classification of mobilizable and conjugative plasmids (35). Our phylogenetic analysis placed PflA506_p0066 (Fig. 5; see also Table S4 in the supplemental material) and all other genes with putative roles in type IV secretion within the MOB_{P6} family (data not shown), which also includes many plasmids from *P. syringae* and species of *Enterobacteriaceae*, including the plant pathogen *E. amylovora*.

Most MOB_{P6} family plasmids have a conserved *oriT*, and the *nic* site (61) and the typical inverted and direct repeats of the region also are present in the *oriT* of pA506 (see Fig. S7 in the supplemental material). The MOB_{P6} plasmids have a VirB/VirD4 system of conjugation, whereby 10 VirB proteins (VirB2 to VirB11) form the conjugation machinery, and VirD4 acts as a type IV coupling protein (T4CP) to the relaxosome, the nucleoprotein complex composed of *oriT*, the relaxase, and auxiliary transfer proteins (60). The conjugal transfer region of pA506 contains putative genes for VirD4 and 8 of the 10 VirB proteins but lacks homologs of *virB1*, which encodes a soluble lytic transglycosylase, and *virB7*, an outer membrane lipoprotein. Intriguingly, the predicted amino acid sequence of an open reading frame (ORF) upstream of *virB2* in pA506 has 11 residues that are identical to a conserved region of the VirB1 proteins in the pPT23A family but lacks an SLT domain present in functional transglycosylases. We speculate that this

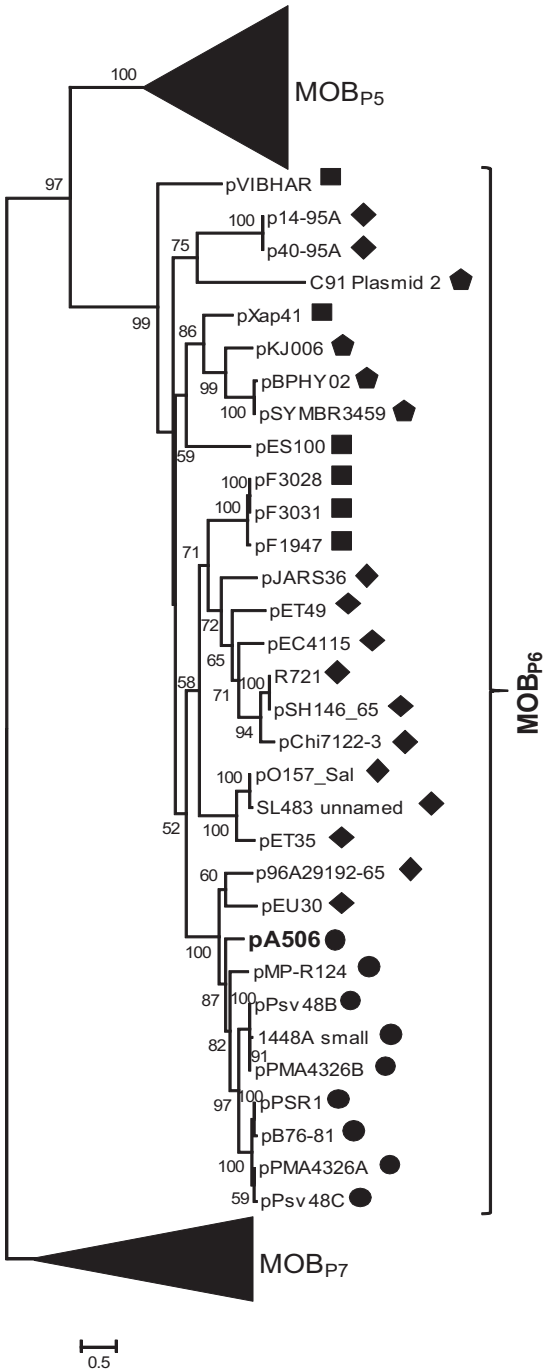

FIG 5 Relaxase-based phylogeny of pA506 and other plasmids in the MOB$_{P6}$ family. The N-terminal 350 aa from PflA506_p0066 were used to identify novel MOB$_{P6}$ family plasmids, as previously described (35). Relaxase sequences from known MOB$_{P5}$, MOB$_{P6}$, and MOB$_{P7}$ family plasmids were also used in generation of this tree. Sequences were aligned by MAFFT L-INS-I, and the LG+G substitution model was identified as the best model using the BIC selection in ProtTest 3. The maximum-likelihood tree was generated using RAxML with the above data as input, and the interior node values indicate the percentage of bootstraps out of 1,000. Bootstrap values below 50 are not shown. Sequences that were significantly shorter than the 350 aa used in the BLASTP search were removed prior to alignment and tree generation. MOB$_{P6}$ family plasmids are in *Pseudomonas* spp. (circles) or species of the *Enterobacteriaceae* (diamonds), other gammaproteobacteria (squares), or betaproteobacteria (pentagons).

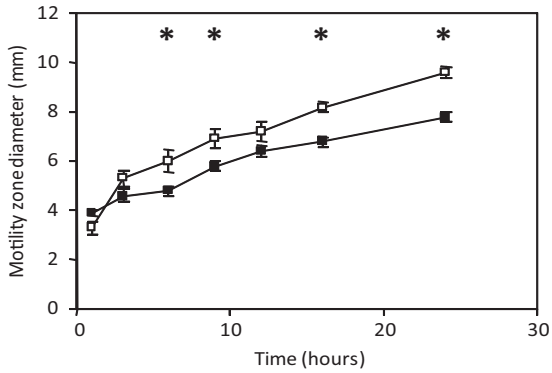

FIG 6 Influence of pA506 on twitching motility of A506. Twitching motility of *Pseudomonas fluorescens* strain A506 (■) and the plasmidless derivative A506-ΔpA506 (□) was assessed on King's medium B solidified with 1% agar. The motility zone was measured over 24 h at the interface of the petri dish and the bottom of the medium. The mean diameter of motility was calculated from five replicate plates per strain; the vertical lines indicate 1 standard error of the mean. Asterisks show time points when the motility of the two strains differed significantly according to Fisher's protected least significant difference at $P = 0.05$.

ORF, which is not annotated in the pA506 sequence, may be a remnant of *virB1*. Within the conjugal transfer region of pA506 are two genes encoding putative outer membrane lipoproteins (PflA506_p0040 and PflA506_p0042) and one for a putative soluble lytic transglycosylase (PflA506_p0052), which possibly could fulfill the roles typically performed by VirB7 and VirB1, respectively. These genes are in or adjacent to the *pil* region described below, which is flanked by *virB*/*virD4* genes in pA506 but is absent from most plasmids in the MOB$_{P6}$ family.

pA506 also contains a cluster of 10 genes, *pilLNOPQRSTVM* (PflA506_p0042 through PflA506_p0051, Fig. 1), which resemble the *pil* regions present in certain conjugative plasmids, such as R64 of *Salmonella enterica* serovar Typhimurium (62), and within integrated conjugative elements (ICEs) on the chromosomes of some strains of *Pseudomonas* spp. (49, 50). These genes are involved in production of thin, flexible sex pili, which have been shown to function in conjugal transfer of plasmid R64 (63) or the ICE PAPI-1 (50) in liquid media. The *pil* cluster of pA506 is identical in organization to that of PAPI-1 of *P. aeruginosa* PA14 (50) and PGFI-1 of *Pseudomonas protegens* Pf-5 (49); all three of these *Pseudomonas pil* regions lack orthologs of *pilU*, which encodes a peptidase required for processing the PilS prepilin. In *P. aeruginosa*, the chromosomally encoded prepilin peptidase PilD provides this processing function and is required for conjugal transfer of PAPI-1 in liquid media (50). *pilD* is also present in the chromosome of *P. fluorescens* A506 (6) and is likely to provide a similar essential function in processing of the PilS prepilin encoded by pA506. The similarity between the *pil* clusters of PAPI-1, plasmid R64, and pA506 suggests that the last encodes type IV pili involved in conjugation rather than twitching motility (64). To identify any potential role of the plasmid-borne *pil* genes in twitching motility, however, we compared A506 to the plasmid-cured derivative A506-ΔpA506. On KB solidified with 1% agar, A506-ΔpA506 and the positive control, *P. aeruginosa* PAO1, were significantly ($P <$ 0.05) more motile than was wild-type A506, which harbors pA506 (Fig. 6; see also Table S5 in the supplemental material). These results demonstrate conclusively that the *pil* genes on pA506 are

not required for twitching motility. The chromosome of A506 has a full complement of *pil* genes, which are responsible for twitching motility of *P. aeruginosa* (64) and probably function similarly in A506. We have not observed a growth difference between wild-type A506 and A506-ΔpA506 in liquid culture (data not shown); therefore, additional research is required to determine the mechanism by which the plasmid reduces twitching motility.

Conjugal transfer of pA506. Conjugal transfer experiments confirmed that pA506 is mobile, not only to other pseudomonads, but also to members of the *Enterobacteriaceae*. Transfer to *P. chlororaphis* O6, *P. fluorescens* SS101, *P. brassicacearum* Q8r1-96, *P. vagans* C9-1, and *E. coli* K-12 was demonstrated using the marked plasmid pA506::*gfp-km-gm*. The plasmid was isolated from transconjugants of each strain, and the BamHI restriction digest pattern was identical to that of the source (Fig. 3). Furthermore, plasmid acquisition by recipients was confirmed with the PCR targeting sequences on the plasmid and also the chromosome of A506 to ensure that the putative transconjugant was not A506 (data not shown). Frequencies of pA506::*gfp-km-gm* transfer, which varied from 10^{-6} to 10^{-7} transconjugants per recipient (data not shown), may not accurately reflect the frequency of pA506 transfer because the morphological changes associated with the *gfp-km-gm* insertion into PflA506_p0022 (see Fig. S6 in the supplemental material) could influence conjugation frequency.

pA506 increases tolerance of A506 to UV irradiation. pA506 contains *rulAB* (PflA506_p0003 and p0004) (Fig. 1; see also Fig. S8 in the supplemental material), which encode the error-prone DNA polymerase V that synthesizes DNA across UV irradiation-induced lesions (65). In *P. syringae*, expression of the *rulAB* operon is controlled by the transcriptional repressor LexA, which binds to a conserved LexA box upstream of the operon (66–68). In response to DNA damage, RecA is activated and interacts with LexA, resulting in self-cleavage of the protein and the induction of the *rulAB* operon. A LexA box was identified 23 nt upstream of *rulA* on pA506. The LexA box sequence is similar to those upstream of *rulAB* on the chromosomes of *P. fluorescens* SS101 and *P. brassicacearum* Q8r1-96, with a common motif of CTGT-N_8-ACAG (6, 66, 68).

rulAB are known to increase the tolerance of *P. syringae* strains to UVB and UVC irradiation, which causes DNA damage (67, 69–72), so we determined if pA506 enhanced UVC tolerance of A506, as expected due to the plasmid-borne *rulAB* operon. To test the sensitivity of our assay, we compared UVC tolerance of A506 to those of *P. fluorescens* SS101 and *P. brassicacearum* Q8r1-96, which have *rulAB*, and to that of *P. chlororaphis* O6, which lacks *rulAB* (6). Considering all experiments, *P. fluorescens* SS101 was significantly ($P < 0.05$) more tolerant of UVC than were the other strains and required an average of 55 J/m^2 to decrease the log survival ratio by 2 units (data not shown). Wild-type A506 and *P. brassicacearum* Q8r1-96 were similar in their tolerance of UVC irradiation and required average doses of 40 J/m^2 and 41 J/m^2, respectively, to decrease the log survival ratio by 2 units (data not shown). *P. chlororaphis* O6 was significantly ($P < 0.05$) more sensitive to UVC irradiation than were the other strains and required an average dose of only 21 J/m^2 to decrease the log survival ratio by 2 units (data not shown). Together, these data confirm the utility of this assay for examining UVC tolerance in pseudomonads.

The assay was used to examine the influence of pA506 on tolerance of the bacterium to UVC irradiation. In repeated assays, A506 was significantly ($P < 0.05$) more tolerant of UVC irradiation than was its plasmid-cured derivative at doses of ≥30 J/m^2 up to 120 J/m^2; 160 J/m^2 was a lethal dose for both the wild type and the plasmidless derivative of A506 (Fig. 7). The level of UVC tolerance of A506 is similar to those of many strains of *P. syringae* (72), and our results are consistent with those from previous studies establishing a role for *rulAB* in UVC tolerance of *P. syringae* (67, 69–72).

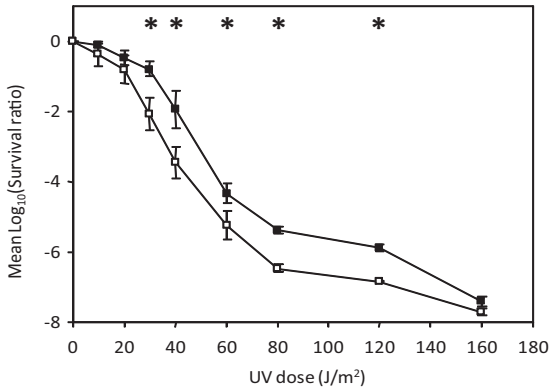

FIG 7 pA506 increased tolerance of A506 to UV irradiation. Tolerance of *Pseudomonas fluorescens* strain A506 (■) and the plasmidless derivative A506-ΔpA506 (□) to UV irradiation was assessed by exposing cells spread on medium to various doses of UVC. Colonies were counted after a 3-day incubation period in the dark. The survival ratio is the population size after exposure to UV divided by the population that was not exposed. The results were averaged from 5 replicate experiments. Vertical bars represent 1 standard error of the mean. Asterisks indicate a significant difference (Fisher's protected least significant difference, $P = 0.05$) between the mean log (survival ratio) of A506 and its plasmidless derivative at various UVC doses.

pA506 did not influence epiphytic fitness on flowers in orchards. On flowers of pear and apple, strains A506 and A506-ΔpA506 established population sizes of ca. 5×10^4 CFU/flower after application (Fig. 8A to C). Environmental conditions during bloom of Bartlett pear were cool and rainy (see Table S2 in the supplemental material). Under these conditions, populations decreased 100-fold by 4 days after application to pear flowers, but thereafter, both A506 and A506-ΔpA506 increased to populations of $>10^5$ CFU/flower (Fig. 8A). Environmental conditions during bloom in both apple flower experiments were warmer and drier than those during pear bloom (see Table S2). In both apple flower experiments, A506 and A506-ΔpA506 achieved mean populations of $\geq 10^5$ CFU/flower within 2 to 3 days after application on apple flowers (Fig. 8B and C). The presence of pA506 in cells of A506 cultured from blossom surfaces on the final sampling date of each experiment was confirmed with the PCR, establishing that the plasmid was maintained by A506 in this environment.

Considering all experiments, mean populations of the plasmidless derivative of A506 were not significantly different than those of the wild type throughout bloom. These results contrast with the results of other studies that have detected roles for plasmids in epiphytic fitness of *Pseudomonas* spp. (69, 73). The different conclusions of these studies are likely due to the varied environmental conditions, plant tissues, plasmids, and strains evaluated. Plasmid size may be one factor. The 330-kb plasmid pQBR103 reduced the fitness of *P. fluorescens* SBW25 in the rhizoplane of sugar beet seedlings (73), which was attributed to the metabolic load imposed by this large plasmid. As plants matured,

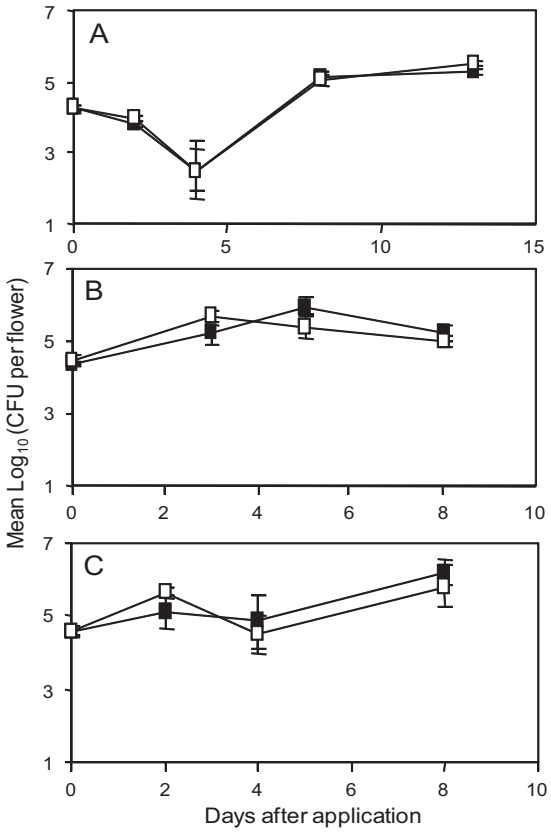

FIG 8 pA506 did not have a detectable influence on epiphytic fitness of *Pseudomonas fluorescens* A506 on pear or apple flowers. Bacterial populations were estimated from flowers on Bartlett pear (A), Gala apple (B), and Red Delicious apple (C) trees at the Botany and Plant Pathology Field Laboratory of Oregon State University near Corvallis, OR. Open flowers were sprayed with 1×10^8 CFU/ml suspensions of A506 (■) or the plasmidless derivative A506-ΔpA506 (□). At 2 to 9 days following inoculation, culturable populations of bacterial strains on the pistillate structures of flowers were estimated by spreading dilutions of tissue washes on selective media. Vertical bars represent 1 standard error of the mean. No significant differences (Fisher's protected least significant difference, $P = 0.05$) between mean population sizes of A506 and its plasmidless derivative were observed.

however, pQBR103 had a negligible influence on the population size of SBW25 on leaves and the rhizosphere (73). Those authors postulated that unidentified context-specific factors encoded by the plasmid may have accounted for the rebound in populations of SBW25 harboring pQBR103 on mature plants. pA506 is less than 20% of the size of pQBR103, and its maintenance may pose a smaller metabolic load on the host bacterium. Accordingly, we have not observed a difference in growth rate between A506 and its plasmidless derivative in culture, and pA506 was also stable in the strain over 100 generations (data not shown).

pA506 afforded greater tolerance to UV radiation than did its plasmidless derivative *in vitro* (Fig. 7), but the intensity of UV-B in orchards in Oregon during the spring may have been too low to injure A506-ΔpA506 and reduce growth relative to the parental strain. Environmental conditions have been shown to influence plasmid-associated fitness in other pseudomonads (69, 73). Transconjugants and wild-type strains of *P. syringae* pv. syringae carrying *rulAB*-bearing plasmids exhibited greater fitness on adaxial surfaces of mango leaves exposed to direct sunlight than did strains without the plasmids, whereas there was no difference in fitness of the strains on the abaxial surface or on leaves under shaded conditions (69). In that study, the presence of a plasmid with *rulAB* increased fitness of bacteria only when exposed to solar radiation on leaves. Similarly, pA506 may confer some fitness benefit to A506 on leaves under conditions of full exposure to solar radiation, but no benefit from the plasmid was observed on flowers in our study, which was done under conditions when A506 is normally deployed as a biological control agent for fire blight.

Conclusions. pA506 has many characteristic features of the pPT23A plasmid family that are widely distributed among pathovars of *P. syringae*, particularly a type IV secretion system involved in conjugative transfer and the *rulAB* genes conferring UV resistance (3). Despite these similarities, pA506 also has many features that are atypical for these plasmids; most notably, it lacks the *repA* gene, which has been considered the defining characteristic of the pPT23A plasmids (46), has atypical plasmid replication and partitioning regions, has a *pil* gene cluster encoding conjugative type IV pili, and carries a distinct complement of cargo genes. Like pA506, other plasmids, such as the well-characterized pR64, carry two sets of conjugative transfer genes (type IV secretion and type IV pili), which serve to expand the conditions under which the plasmids are self-transmissible (62, 63). Given the diversity of habitats occupied by *P. fluorescens*, the flexibility to transfer genetic material under a broad set of environmental conditions may be particularly important. Whereas many members of the pPT23A family confer virulence traits as well as streptomycin or copper resistance that enables the host bacterium to survive chemical control measures used for plant disease management (3, 39), pA506 does not carry known genes for virulence or antibiotic or heavy metal resistance.

The atypical G+C content of pA506 relative to the A506 chromosome suggests that the plasmid was acquired recently in the evolutionary history of the strain. Based on the phylogenetic relationships of all CDSs having a conjugative function to plasmid-borne genes in the *Enterobacteriaceae* and the average pA506 G+C content of 53%, which is similar to that of the *Enterobacteriaceae*, it is tempting to speculate that plasmids in that large group of gammaproteobacteria may be ancestral to pA506. Indeed, our relaxase-based phylogeny places the pA506 within the larger MOB_{P6} family that includes many plasmids from the *Enterobacteriaceae* (Fig. 5). In contrast, genes conferring functions in plasmid replication and partitioning may have a distinct origin, possibly a member of the alphaproteobacteria. Several other *Pseudomonas* plasmids have replication and partitioning loci similar to those in pA506, including pPT14-32, where these regions are contiguous. We speculate that these regions may have been acquired together and been separated upon the subsequent acquisition of the *rulAB* and other intervening sequences between *oriV* and the *par* region of pA506. As additional plasmid sequences become available, it is likely that a clearer picture of the evolution of pA506 will emerge, but at present, the plasmid appears to have a mosaic structure composed of blocks of genes having distinct origins.

We estimate that approximately 4×10^{16} cells of A506 have been released into environment during bloom of apple and pear orchards in a single year based on agricultural use data for BlightBan A506 (7). We tested the fitness of A506 and A506-ΔpA506 on flowers because that is the tissue colonized for biological control of fire blight (7–9). We did not observe a correlation between epiphytic fitness and carriage of pA506 on flowers. While pA506 is

mobile and may be transferred and maintained in other bacteria residing in orchards, the lack of known genetic determinants for virulence, toxicity, or tolerance to antibiotics and/or copper reduces the potential impact of its transfer. If the plasmid pA506 was acquired by plant-pathogenic bacteria, it is unlikely that efficacy of current disease management practices would be diminished.

ACKNOWLEDGMENTS

We thank Jennifer Lee and Rachel Blumhagen for technical assistance, Todd Temple for selecting A506 pA506::*gfp-km-gm*, Steve Lindow for providing *P. fluorescens* A506, Anne Anderson for providing *P. chlororaphis* O6, Dave Weller for providing *P. brassicacearum* Q8r1-96, Jos Raaijmakers for providing *P. fluorescens* SS101, and Carol Ishimaru for providing *P. vagans* C9-1.

This work was supported by grants 2008-35600-18770 and 2012-67013-19392 from the USDA National Institute of Food and Agriculture.

REFERENCES

1. **Fullbrook PD, Elson SW, Slocombe B.** 1970. R-factor mediated beta-lactamase in *Pseudomonas aeruginosa*. Nature **226:**1054–1056.
2. **Gootz TD.** 2010. The global problem of antibiotic resistance. Crit. Rev. Immunol. **30:**79–93.
3. **Sundin GW.** 2007. Genomic insights into the contribution of phytopathogenic bacterial plasmids to the evolutionary history of their hosts. Annu. Rev. Phytopathol. **45:**129.
4. **Stavrinides J, Guttman DS.** 2004. Nucleotide sequence and evolution of the five-plasmid complement of the phytopathogen *Pseudomonas syringae* pv. maculicola ES4326. J. Bacteriol. **186:**5101–5115.
5. **Dennis JJ.** 2005. The evolution of IncP catabolic plasmids. Curr. Opin. Biotechnol. **16:**291–298.
6. **Loper JE, Hassan KA, Mavrodi DV, Davis EW, II, Lim CK, Shaffer BT, Elbourne LDH, Stockwell VO, Hartney SL, Breakwell K, Henkels MD, Tetu SG, Rangel LI, Kidarsa TA, Wilson NL, van de Mortel JE, Song C, Blumhagen R, Radune D, Hostetler JB, Brinkac LM, Durkin AS, Kluepfel DA, Wechter WP, Anderson AJ, Kim YC, Pierson LS, III, Pierson EA, Lindow SE, Kobayashi DY, Raaijmakers JM, Weller DM, Thomashow LS, Allen AE, Paulsen IT.** 2012. Comparative genomics of plant-associated *Pseudomonas* spp.: insights into diversity and inheritance of traits involved in multitrophic interactions. PLoS Genet. **8:**e1002784. doi:10.1371/journal.pgen.1002784.
7. **Stockwell VO, Stack JP.** 2007. Using *Pseudomonas* spp. for integrated biological control. Phytopathology **97:**244–249.
8. **Lindow SE, Suslow TV.** 2003. Temporal dynamics of the biological control agent *Pseudomonas fluorescens* strain A506 in flowers in inoculated pear trees. Phytopathology **93:**727–737.
9. **Johnson KB, Stockwell VO, Sawyer TL.** 2004. Adaptation of fire blight forecasting to optimize the use of biological controls. Plant Dis. **88:**41–48.
10. **Lindow SE.** 1984. Integrated control and role of antibiosis in biological control of fire blight and frost injury, p 83–115. *In* Windels C, Lindow SE (ed), Biological control on the phylloplane. APS Press, Minneapolis, MN.
11. **Wilson M, Lindow SE.** 1993. Interactions between the biological control agent *Pseudomonas fluorescens* A506 and *Erwinia amylovora* in pear blossoms. Phytopathology **83:**117–123.
12. **Casavant NC, Thompson D, Beattie GA, Phillips GJ, Halverson LJ.** 2003. Use of a site-specific recombination-based biosensor for detecting bioavailable toluene and related compounds on roots. Environ. Microbiol. **5:**238–249.
13. **Stiner L, Halverson LJ.** 2002. Development and characterization of a green fluorescent protein-based bacterial biosensor for bioavailable toluene and related compounds. Appl. Environ. Microbiol. **68:**1962–1971.
14. **Temple T, Stockwell VO, Loper JE, Johnson KB.** 2004. Bioavailability of iron to *Pseudomonas fluorescens* strain A506 on flowers of pear and apple. Phytopathology **94:**1286–1294.
15. **Wright CA, Beattie GA.** 2004. *Pseudomonas syringae* pv. *tomato* cells encounter inhibitory levels of water stress during the hypersensitive response of *Arabidopsis thaliana*. Proc. Natl. Acad. Sci. U. S. A. **101:**3269–3274.
16. **Dianese AC, Ji PS, Wilson M.** 2003. Nutritional similarity between leaf-associated nonpathogenic bacteria and the pathogen is not predictive of efficacy in biological control of bacterial spot of tomato. Appl. Environ. Microbiol. **69:**3484–3491.
17. **Lindow SE, Brandl MT.** 2003. Microbiology of the phyllosphere. Appl. Environ. Microbiol. **69:**1875–1883.
18. **Mercier J, Lindow SE.** 2000. Role of leaf surface sugars in colonization of plants by bacterial epiphytes. Appl. Environ. Microbiol. **66:**369–374.
19. **Pusey PL, Curry EA.** 2004. Temperature and pomaceous flower age related to colonization by *Erwinia amylovora* and antagonists. Phytopathology **94:**901–911.
20. **Monier JM, Lindow SE.** 2005. Aggregates of resident bacteria facilitate survival of immigrant bacteria on leaf surfaces. Microb. Ecol. **49:**343–352.
21. **Monier JM, Lindow SE.** 2005. Spatial organization of dual-species bacterial aggregates on leaf surfaces. Appl. Environ. Microbiol. **71:**5484–5493.
22. **Lowder M, Unge A, Maraha N, Jansson JK, Swiggett J, Oliver JD.** 2000. Effect of starvation on the viable-but-nonculturable state on green fluorescent protein (GFP) fluorescence in GFP-tagged *Pseudomonas fluorescens* A506. Appl. Environ. Microbiol. **66:**3160–3165.
23. **Bunker ST BT, Oliver JD.** 2004. Effects of temperature on detection of plasmid or chromosomally encoded gfp- and lux-labeled *Pseudomonas fluorescens* in soil. Environ. Biosafety Res. **3:**83–90.
24. **Sambrook J, Russell D.** 2001. Molecular cloning: a laboratory manual, 3rd ed. Cold Spring Harbor Laboratory Press, Cold Spring Harbor, NY.
25. **King EO, Ward MK, Raney DE.** 1954. Two simple media for the demonstration of pyocyanin and fluorescin. J. Lab. Clin. Med. **44:**301–307.
26. **Tang X, Lu BF, Pan SQ.** 1999. A bifunctional transposon mini-Tn*5gfp-km* which can be used to select for promoter fusions and report gene expression levels in *Agrobacterium tumefaciens*. FEMS Microbiol. Lett. **179:**37–42.
27. **Sievers F, Wilm A, Dineen D, Gibson TJ, Karplus K, Li W, Lopez R, McWilliam H, Remmert M, Soding J, Thompson JD, Higgins DG.** 2011. Fast, scalable generation of high-quality protein multiple sequence alignments using Clustal Omega. Mol. Syst. Biol. **7:**539. doi:10.1038/msb.2011.75.
28. **Price MN, Dehal PS, Arkin AP.** 2010. FastTree 2—approximately maximum-likelihood trees for large alignments. PLoS One **5:**e9490. doi:10.1371/journal.pone.0009490.
29. **Katoh K, Standley DM.** 2013. MAFFT multiple sequence alignment software version 7: improvements in performance and usability. Mol. Biol. Evol. **30:**772–780.
30. **Darriba D, Taboada GL, Doallo R, Posada D.** 2011. ProtTest 3: fast selection of best-fit models of protein evolution. Bioinformatics **27:**1164–1165.
31. **Stamatakis A.** 2006. RAxML-VI-HPC: maximum likelihood-based phylogenetic analyses with thousands of taxa and mixed models. Bioinformatics **22:**2688–2690.
32. **Silvestro D, Michalak I.** 2012. raxmlGUI: a graphical front-end for RAxML. Org. Divers. Evol. **12:**335–337.
33. **Tamura K, Peterson D, Peterson N, Stecher G, Nei M, Kumar S.** 2011. MEGA5: molecular evolutionary genetics analysis using maximum likelihood, evolutionary distance, and maximum parsimony methods. Mol. Biol. Evol. **28:**2731–2739.
34. **Stöver BC, Müller KF.** 2010. TreeGraph 2: combining and visualizing evidence from different phylogenetic analyses. BMC Bioinformatics **11:**7. doi:10.1186/1471-2105-11-7.
35. **Garcillán-Barcia MP, Francia MV, de la Cruz F.** 2009. The diversity of conjugative relaxases and its application in plasmid classification. FEMS Microbiol. Rev. **33:**657–687.
36. **Okonechnikov K, Golosova O, Fursov M.** 2012. Unipro UGENE: a unified bioinformatics toolkit. Bioinformatics **28:**1166–1167.
37. **Edgar RC.** 2004. MUSCLE: multiple sequence alignment with high accuracy and high throughput. Nucleic Acids Res. **32:**1792–1797.
38. **Waterhouse AM, Procter JB, Martin DMA, Clamp M, Barton GJ.** 2009. Jalview version 2—a multiple sequence alignment editor and analysis workbench. Bioinformatics **25:**1189–1191.
39. **Sundin GW, Jones AL, Fulbright DW.** 1989. Copper resistance in *Pseudomonas syringae* pv. *syringae* from cherry orchards and its associated transfer *in vitro* and *in planta* with a plasmid. Phytopathology **79:**861–865.
40. **Langley RA, Kado CI.** 1972. Studies on *Agrobacterium tumefaciens*. Conditions for mutagenesis by N-methyl-N′-nitrosoguanidine and relationships of *A. tumefaciens* mutants to crown gall tumor induction. Mutat. Res. **14:**277–286.
41. **Gallant CV, Daniels C, Leung JM, Ghosh AS, Young KD, Kotra LP,**

Burrows LL. 2005. Common beta-lactamases inhibit bacterial biofilm formation. Mol. Microbiol. **58:**1012–1024.
42. **Whistler CA, Stockwell VO, Loper JE.** 2000. Lon protease influences antibiotic production and UV tolerance of *Pseudomonas fluorescens* Pf-5. Appl. Environ. Microbiol. **66:**2718–2725.
43. **Stockwell VO, Johnson KB, Sugar D, Loper JE.** 2002. Antibiosis contributes to biological control of fire blight by *Pantoea agglomerans* strain Eh252 in orchards. Phytopathology **92:**1202–1209.
44. **Sundin GW, Mayfield CT, Zhao Y, Gunasekera TS, Foster GL, Ullrich MS.** 2004. Complete nucleotide sequence and analysis of pPSR1 (72,601 bp), a pPT23A-family plasmid from *Pseudomonas syringae* pv. *syringae* A2. Mol. Genet. Genomics **270:**462–476.
45. **Joardar V, Lindeberg M, Jackson RW, Selengut J, Dodson R, Brinkac LM, Daugherty SC, DeBoy R, Durkin AS, Giglio MG, Madupu R, Nelson WC, Rosovitz MJ, Sullivan S, Crabtree J, Creasy T, Davidsen T, Haft DH, Zafar N, Zhou L, Halpin R, Holley T, Khouri H, Feldblyum T, White O, Fraser CM, Chatterjee AK, Cartinhour S, Schneider DJ, Mansfield J, Collmer A, Buell CR.** 2005. Whole-genome sequence analysis of *Pseudomonas syringae* pv. phaseolicola 1448A reveals divergence among pathovars in genes involved in virulence and transposition. J. Bacteriol. **187:**6488–6498.
46. **Ma Z, Smith JJ, Zhao Y, Jackson RW, Arnold DL, Murillo J, Sundin GW.** 2007. Phylogenetic analysis of the pPT23A plasmid family of *Pseudomonas syringae*. Appl. Environ. Microbiol. **73:**1287–1295.
47. **Foster GC, McGhee GC, Jones AL, Sundin GW.** 2004. Nucleotide sequences, genetic organization, and distribution of pEU30 and pEL60 from *Erwinia amylovora*. Appl. Environ. Microbiol. **70:**7539–7544.
48. **Kube M, Migdoll AM, Müller I, Kuhl H, Beck A, Reinhardt R, Geider K.** 2008. The genome of *Erwinia tasmaniensis* strain Et1/99, a nonpathogenic bacterium in the genus *Erwinia*. Environ. Microbiol. **10:**2211–2222.
49. **Mavrodi DV, Loper JE, Paulsen IT, Thomashow LS.** 2009. Mobile genetic elements in the genome of the beneficial rhizobacterium *Pseudomonas fluorescens* Pf-5. BMC Microbiol. **9:**8. doi:10.1186/1471-2180-9-8.
50. **Carter MQ, Chen J, Lory S.** 2010. The *Pseudomonas aeruginosa* pathogenicity island PAPI-1 is transferred via a novel type IV pilus. J. Bacteriol. **192:**3249–3258.
51. **Michel-Briand Y, Baysse C.** 2002. The pyocins of *Pseudomonas aeruginosa*. Biochimie **84:**499–510.
52. **Kolatka K, Kubik S, Rajewska M, Konieczny I.** 2010. Replication and partitioning of the broad-host-range plasmid RK2. Plasmid **64:**119–134.
53. **Kwong SM, Yeo CC, Chuah D, Poh CL.** 1998. Sequence analysis of plasmid pRA2 from *Pseudomonas alcaligenes* NCIB 9867 (P25X) reveals a novel replication region. FEMS Microbiol. Lett. **158:**159–165.
54. **Garcillan-Barcia MP, Alvarado A, de la Cruz F.** 2011. Identification of bacterial plasmids based on mobility and plasmid population biology. FEMS Microbiol. Rev. **35:**936–956.
55. **Wu M, Zampini M, Bussiek M, Hoischen C, Diekmann S, Hayes F.** 2011. Segrosome assembly at the pliable *parH* centromere. Nucleic Acids Res. **39:**5082–5097.
56. **Szardenings F, Guymer D, Gerdes K.** 2011. ParA ATPases can move and position DNA and subcellular structures. Curr. Opin. Microbiol. **14:**712–718.
57. **Makarova KS, Grishin NV, Koonin EV.** 2006. The HicAB cassette, a putative novel, RNA-targeting toxin-antitoxin system in archaea and bacteria. Bioinformatics **22:**2581–2584.
58. **Jørgensen MG, Pandey DP, Jaskolska M, Gerdes K.** 2009. HicA of *Escherichia coli* defines a novel family of translation-independent mRNA interferases in bacteria and archaea. J. Bacteriol. **191:**1191–1199.
59. **Bartosik AA, Mierzejewska J, Thomas CM, Jagura-Burdzy G.** 2009. ParB deficiency in *Pseudomonas aeruginosa* destabilizes the partner protein ParA and affects a variety of physiological parameters. Microbiology **155:**1080–1092.
60. **Alvarez-Martinez CE, Christie PJ.** 2009. Biological diversity of prokaryotic type IV secretion systems. Microbiol. Mol. Biol. Rev. **73:**775–808.
61. **Komano T, Fujitani S, Funayama N, Kanno A, Nisioka T.** 1987. Genetic and physical characterization of the plasmid R721. Jpn. J. Genet. **62:**528–535.
62. **Sampei G, Furuya N, Tachibana K, Saitou Y, Suzuki T, Mizobuchi K, Komano T.** 2010. Complete genome sequence of the incompatibility group I1 plasmid R64. Plasmid **64:**92–103.
63. **Komano T, Yoshida T, Narahara K, Furuya N.** 2000. The transfer region of IncI1 plasmid R64: similarities between R64 *tra* and *Legionella icm/dot* genes. Mol. Microbiol. **35:**1348–1359.
64. **Mattick JS.** 2002. Type IV pili and twitching motility. Annu. Rev. Microbiol. **56:**289–314.
65. **Patel M, Jiang Q, Woodgate R, Cox MM, Goodman MF.** 2010. A new model for SOS-induced mutagenesis: how RecA protein activates DNA polymerase V. Crit. Rev. Biochem. Mol. Biol. **45:**171–184.
66. **Erill I, Escribano M, Campoy S, Barbé J.** 2003. *In silico* analysis reveals substantial variability in the gene contents of the gamma proteobacteria LexA-regulon. Bioinformatics **19:**2225–2236.
67. **Feil H, Feil WS, Chain P, Larimer F, Dibartoio G, Copeland A, Lykidis A, Trong S, Nolan M, Goltsman E, Thiel J, Malfatti S, Loper JE, Lapidus A, Detter JC, Land M, Richardson PM, Kyrpides NC, Ivanova N, Lindow SE.** 2005. Comparison of the complete genome sequences of *Pseudomonas syringae* pv. *syringae* B728a and pv. *tomato* DC3000. Proc. Natl. Acad. Sci. U. S. A. **102:**11064–11069.
68. **Mazón G, Erill I, Campoy S, Cortés P, Forano E, Barbé J.** 2004. Reconstruction of the evolutionary history of the LexA-binding sequence. Microbiology **150:**3783–3795.
69. **Cazorla FM, Codina JC, Abad C, Arrebola E, Torés JA, Murillo J, Pérez-García A, Vicente A.** 2008. 62-kb plasmids harboring *rulAB* homologues confer UV-tolerance and epiphytic fitness to *Pseudomonas syringae* pv. *syringae* mango isolates. Microb. Ecol. **56:**283–291.
70. **Gunasekera TS, Sundin GW.** 2006. Role of nucleotide excision repair and photoreactivation in the solar UVB radiation survival of *Pseudomonas syringae* pv. *syringae* B728a. J. Appl. Microbiol. **100:**1073–1083.
71. **Jacobs JL, Carroll TL, Sundin GW.** 2005. The role of pigmentation, ultraviolet radiation tolerance, and leaf colonization strategies in the epiphytic survival of phyllosphere bacteria. Microb. Ecol. **49:**104–113.
72. **Sundin GW, Jacobs JL, Murillo J.** 2000. Sequence diversity of *rulA* among natural isolates of *Pseudomonas syringae* and effect on function of *rulAB*-mediated UV radiation tolerance. Appl. Environ. Microbiol. **66:**5167–5173.
73. **Lilley AK, Bailey MJ.** 1997. Impact of plasmid pQBR103 acquisition and carriage on the phytosphere fitness of *Pseudomonas fluorescens* SBW25: burden and benefit. Appl. Environ. Microbiol. **63:**1584–1587.
74. **Alikhan NF, Petty NK, Ben Zakour NL, Beatson SA.** 2011. BLAST Ring Image Generator (BRIG): simple prokaryote genome comparisons. BMC Genomics **12:**402. doi:10.1186/1471-2164-12-402.
75. **Holloway BW.** 1955. Genetic recombination in *Pseudomonas aeruginosa*. J. Gen. Microbiol. **13:**572–581.
76. **Raaijmakers JM, Weller DM.** 2001. Exploiting genotypic diversity of 2,4-diacetylphloroglucinol-producing *Pseudomonas* spp.: characterization of superior root-colonizing *P. fluorescens* strain Q8r1-96. Appl. Environ. Microbiol. **67:**2545–2554.
77. **Tucker B, Radtke C, Kwon SI, Anderson AJ.** 1995. Suppression of bioremediation by *Phanerochaete chrysosporium* by soil factors. J. Hazard. Mater. **41:**251–265.
78. **de Souza JT, de Boer M, de Waard P, van Beek TA, Raaijmakers JM.** 2003. Biochemical, genetic, and zoosporicidal properties of cyclic lipopeptide surfactants produced by *Pseudomonas fluorescens*. Appl. Environ. Microbiol. **69:**7161–7172.
79. **Ishimaru CA, Klos EJ, Brubaker RR.** 1988. Multiple antibiotic production by *Erwinia herbicola*. Phytopathology **78:**746–750.
80. **Smits THM, Rezzonico F, Kamber T, Blom J, Goesmann A, Ishimaru CA, Frey JE, Stockwell VO, Duffy B.** 2011. Metabolic versatility and antibacterial metabolite biosynthesis are distinguishing genomic features of the fire blight antagonist *Pantoea vagans* C9-1. PLoS One **6:**e22247. doi:10.1371/journal.pone.0022247.